

NASA Technical Memorandum 79229

FREE JET PHENOMENA IN A 90°-SHARP  
EDGE INLET GEOMETRY

(NASA-TM-79229) FREE JET PHENOMENA IN A 90  
DEGREE-SHARP EDGE INLET GEOMETRY (NASA)  
30 p HC A03/MF A01 CSCL 20D

N79-31526

Unclas  
G3/34 31982

R. C. Hendricks  
Lewis Research Center  
Cleveland, Ohio



Prepared for the  
International Cryogenic Engineering Conference and the  
International Cryogenic Materials Conference  
Sponsored by the National Bureau of Standards  
Madison, Wisconsin, August 21-24, 1979

FREE PHENOMENA IN A 90° - SHARP  
EDGE INLET GEOMETRY

R. C. Hendricks

National Aeronautics and Space Administration  
Lewis Research Center  
Cleveland, Ohio 44135

ABSTRACT

Under certain conditions, inlets with a sharp edge or geometric corner have been shown to exhibit sufficiently strong separation effects to permit the working fluid to flow through the duct as if it were a "free jet."

Mass limiting flow data and associated pressure profiles for tubes of 53, 64, 73, and 105 L/D with a 90° - sharp edge or orifice type inlet were taken and compared to Borda type inlet data to determine bounds of the "free jet" phenomena. For smooth tubes the limits appear to be one dimensional and dependent only on inlet stagnation conditions. The upper L/D boundary is related by

$$P_{R_0} \approx C T_{R_0}^7$$

$$C \approx 1.8 \times 10^{-4} (L/D)^{2.5}$$

where  $P_{R_0} = P_0/P_c$  is reduced stagnation pressure and  $T_{R_0} = T_0/T_c$  is reduced stagnation temperature (for fluid nitrogen,  $T_c = 126.3 \text{ K}$  and  $P_c = 3.417 \text{ MPa}$ ). The lower bound appears to be saturation conditions at the inlet.

Similar "free jet" effects were found for fluid hydrogen indicating that fluid jetting may be common to all fluids flowing through 90° - sharp edge inlet geometries.

INTRODUCTION

The stability of seals, bearings and shaft dampers depends critically on the pressure profiles within the clearance passages. The pressure profiles which provide the restoring forces and stiffness in some passages are critically dependent on inlet geometry and fluid stagnation pressure and temperature. In nearly all cases, simple geometries or combinations of simple geometries are used.

The 90° orifice inlet type is one of the most common sharp edge inlet geometries, yet represents a very strong degree of discontinuity in the streamline as

can be noted from the potential flow solutions for several simple two dimensional geometries, found in references 1 and 2.

The simple inlet geometry which causes a full reversal in the streamline and represents the strongest degree of discontinuity is called the Borda inlet. The pressure profiles and mass limiting flow characteristics for a 53 L/D Borda tube were investigated in reference 3 and extended to 64, 73, and 105 L/D in reference 4, using fluids nitrogen and hydrogen over a large range of inlet stagnation conditions. Under certain conditions ( $P_o, T_{o1}$ ) the discontinuity (separation) was sufficiently strong to permit the fluid to flow through the tube as if it were a free jet for over 105 L/D, as evidenced by the "flat" pressure profile and illustrated on figure 1. Under these conditions, the pressure plummets to below the saturation pressure followed by an initial recompression (recovery) (recovery and recompression will be used interchangeably until the physical mechanism is better understood) and remains nearly constant throughout the remainder of the tube - actually the pressure increased over the length to nearly  $P_{sat}(T_{o1})$  at the exit. The contrast with the conventional gaseous case is substantial. For other conditions ( $P_o, T_{o2}$ ) the pressure would plummet and recover as before but then a zone of secondary recompression (recovery) would occur somewhere within the tube and the pressure would drop to near  $P_{sat}(T_{o2})$  at the exit.

Since the occurrence of the free jet and the movement of the secondary recompression zone can affect large changes in axial pressure profiles (large changes in forces) it is necessary to know under what conditions one can expect the pressure profile to be (i) "flat", (ii) recompressed within the tube or, (iii) behave like a gas. In reference 3 it was found that gas like behavior can be expected where  $T_{Ro} > 1.2$ , and a criterion was proposed to determine where secondary recompression occurred within the 53 L/D Borda tube. The expression for this locus was given as:

$$P_{Ro} = C T_{Ro}^7 \quad (1)$$

where

$$C = 3.6 \quad (2)$$

In reference 4 three constraints were found: L/D, minimum stagnation pressure and surface roughness ( $\epsilon$ ) which govern the secondary recompression locus of eq. (1). The effect of L/D on the geometric constant C was investigated at 64, 73 and 105 L/D and with the 53 L/D data of reference 3. It was found for smooth tubes that:

$$C(L/D, \epsilon) = 1.7 \times 10^{-4} (L/D)^{2.5} \quad (3)$$

and from limited data, roughness ( $\epsilon$ ) increased the effective  $L/D$ , i.e., increased  $C$ , however no quantitative assessment was given. The minimum stagnation pressure is the saturation or pseudo-saturation pressure and is given by the criterion

$$P_{o\min} = \begin{cases} P_{\text{sat}}(T_o) & T_{R_o} \leq 1 \\ P_{\text{pseudo}} & T_{R_o} > 1 \end{cases} \quad (4)$$

For pressures greater than  $P_{R_o}$  calculated by eqs. (1) and (3), and greater than  $P_{o\min}$  determined by eq. (4), the free jet phenomena can be expected to occur and the pressure profile will be "flat;" for pressures less than those calculated from eqs. (1) to (4), secondary recompression will occur within the tube.

It should be noted that the occurrence of the secondary recompression zone within the tube depends only on inlet stagnation conditions and the geometric parameter  $C$ , but the influence of inlet geometry is unknown.

In this paper we propose to extend the work of reference 4 to the  $90^\circ$ -sharp edge inlet. As in references 3 and 4, we elected to study the effect of  $L/D$  in smooth (polished) tubes, as polished surfaces are common in seals and bearings.

The primary working fluid is nitrogen with some runs made with fluid hydrogen. These data will enable one to extend some results to other fluids.

#### APPARATUS AND INSTRUMENTATION

The basic flow facility was of the blowdown type and is described in detail in reference 5. A photograph of the installed 53  $L/D$ - $90^\circ$ -sharp edge inlet test section (fig. 2) illustrates the pressure taps and associated plumbing. The flow was upward, around the U and downward through the test section. The flow rates were metered using a venturi flowmeter located in the bottom of the storage tank. Inlet stagnation conditions were measured in a mixing chamber not shown in figure 2.

The test sections consisted of three components, the  $90^\circ$  sharp edge inlet (fig. 3), an extension piece and the fixed diffuser which were very carefully assembled to form a tube (fig. 4). The length of the extension tube was varied to produce the desired  $L/D$ . Photographs of these test sections are given as figures 5(a) to (d). The apparatus and instrumentation is essentially that used in reference 3. Only a brief description will be given here for convenience. All test sections had several local pressure taps, three stagnation pressures, and a backpressure which were used to establish the axial pressure profiles. The tap locations are given in table 1.

The bore of test section was hand lapped using fine emery paper and cutting oil. The surface was smooth but eccentricities and discontinuities at the joints were evident. For expediency the joints were tolerated.

## RESULTS AND DISCUSSION

The procedure will be to first establish an L/D constraint as the upper limit to free jet flow in terms of the loci for incipient secondary recompression (recovery), and then determine some results which will permit extension to other fluids.

### L/D Constraint

For each of the four test sections (L/D = 53, 64, 73, and 105), see figures 2 to 5 and table I, critical mass flow rate and pressure profiles will be used to determine the range of inlet stagnation conditions where incipient secondary recompression (recovery) occurs within the tube with a 90° sharp edge inlet. Each of the figures will be generalized through the use of reducing parameters or corresponding states parameters.

### 53 L/D 90°-Sharp Edge Inlet Tube

The most extensive set of critical mass flux and pressure profile data are for the 53 L/D 90°-sharp edge inlet tube. Figure 6 illustrates the variation of critical mass flux as a function of reduced pressure for several isotherms ranging to  $T_{R0} = 1.09$  and gas. For a given inlet stagnation isotherm, the departure of the pressure profiles from the "flat" monotone rise throughout the tube length signals the incipience or appearance of the zone of secondary recompression for that isotherm; care must be taken to determine those inlet stagnation conditions under which incipience occurs. Such typical profile sets are illustrated in figures 7 and 9 schematically on figure 1. For the nominally 109.7 K isotherm, the pressure drops to  $P_{sat}(T_0)/4$  followed by an initial recompression to  $3P_{sat}(T_0)/4$ , and increases in a monotone manner toward  $P_{sat}(T_0)$  at the exit. Entropy is a more satisfactory criteria but more difficult to visualize. As the inlet stagnation pressure is decreased, the zone of secondary recompression occurs within the tube; further decreases in stagnation pressure forces the merger of initial and secondary zones of recompression.

From a multiplicity of such pressure profile sets as figure 7 (one set for each isotherm), the locus of incipient secondary recompression can then be constructed as shown in figure 6. Above the locus a free jet occurs and below the locus, secondary recompression occurs somewhere within the tube. It is quite evident

that while the pressure profiles can change significantly, there appears little change in the critical mass flux. The data set is given as table II.

#### 64 L/D 90°-Sharp Edge Inlet Tube

Inserting a 5.38 cm uninstrumented tube between the 90°-sharp edge inlet and the fixed diffuser geometry, increased the L/D from 53 to 64, see figures 3 to 5. Typical critical mass flux and pressure profiles are given as figures 8 and 9, respectively. As our main goal is to determine the locus of incipient secondary recompression, these data are limited but sufficient to construct the locus on figure 8. The data set is given as table III.

#### 73 L/D 90°-Sharp Edge Inlet Tube

Inserting a 9.98 cm extension tube increased the L/D from 53 to 73, see figures 3 to 5. Pressure profiles and critical mass flux at given stagnation isotherms were again used to establish the incipient secondary recompression locus. The locus was then constructed on figure 10. The data set is given as table IV, with characteristic pressure profiles as figure 11.

#### 105 L/D 90°-Sharp Edge Inlet Tube

Preliminary results herein and the Borda tube results of references 3 and 4 indicated that for the 85 K isotherm, a 25.1 cm extension tube can be used and a free jet sustained in our facility to 105 L/D. Typical pressure profiles are illustrated in figure 12.

Using these data and the critical mass flux data of figure 13, an incipient secondary recompression locus was estimated for the 105 L/D 90°-sharp edge inlet tube. The data are given in table V.

Using figures 6, 8, 10, and 13, one can now construct figure 14(a) to (d) which represents the relation between incipient secondary recompression and inlet stagnation, pressure, and temperature. For direct comparison, similar data are displayed on figures 14(a) to (d) which represent the incipient secondary recompression locus for the Borda inlet, from reference 4. The reader is first cautioned that exact points of incipience were not possible for such points not only depend on  $P_0$  and  $T_0$  but the interaction of the free jet with the tube boundaries, a stability problem; and second that the stagnation pressure range between incipience and no incipience was usually large, giving a certain arbitrariness to the selection of the points on figure 14. These selected results are best represented by the form

$$P_{R_0} = C(L/D, \epsilon) T_{R_0}^n \quad (5)$$

where  $6.5 \leq n \leq 8.5$  and based on the data herein and those of reference 4, we selected  $n = 7$ .

Using the intercepts of figure 14, the values of  $C$  can be found as a function of  $L/D$  for smooth tubes. Figure 15 depicts this relation

$$C(L/D, \epsilon) = C_1 (L/D)^m \quad (6)$$

where  $2.5 < m < 3.5$  and selecting  $m = 2.5$  gives  $C_1 = 1.8 \times 10^{-4}$ . Eqs. (5) and (6) established an  $L/D$  constraint on inlet stagnation conditions for smooth  $90^\circ$ -sharp edge inlet tubes; however, it now appears that roughness plays a greater role than perceived, and is discussed in reference 4.

A comparison of reduced mass flux data for the  $90^\circ$ -sharp edge and Borda type inlets, figure 16, reveals some differences at low reduced temperatures; however the effect appears less pronounced as  $T_{R_0} \rightarrow 1$ . And for gases, the data of reference 6 at  $L/D = 2$ , indicate there to be perhaps 5 percent difference in mass flow rate between the  $90^\circ$ -sharp edge and Borda geometries.

#### Extension to Other Fluids

The extension of these results to other fluids is a necessary step toward any general analysis. In an attempt toward generalization several data points were taken with fluid hydrogen in the 53  $L/D$   $90^\circ$ -sharp edge inlet tube, table VI. Figure 17 indicates typical pressure profiles which have the same general form as for fluid nitrogen, indicating that a fluid jet can be sustained in fluid hydrogen. Further, using the corresponding states arguments of references 7 to 9, it is implied that such jetting phenomena are characteristic of all simple fluids. Both nitrogen and hydrogen data indicate that the jetting effect can be quite strong even where the inlet stagnation temperature approaches the thermodynamic critical temperature (for hydrogen,  $P_c = 1.293$  MPa,  $T_c = 33$  K). It should be noted however that the reduced inlet stagnation pressure is quite high, i. e., to 6, which is over 2 1/2 times larger than our system will permit for fluid nitrogen. This of course is another reason to take data with fluid hydrogen, namely to at least double the range of application of the reduced results determined with fluid nitrogen.

The reduced critical mass flux data appear as figure 18, as a function of reduced stagnation pressure for selected stagnation isotherms. A comparison of the hydrogen and nitrogen data indicate that the phenomena encountered in the 53  $L/D$   $90^\circ$ -sharp edge inlet tube follow the applied principles of corresponding

states. As such, critical mass flux results determined with fluid nitrogen are applicable to fluid hydrogen and vice versa.

For pressure profiles, the correspondence is not so good. With fluid hydrogen at  $P_{R_0} < 1$  system control and measurement become quite difficult. Near  $T_{R_0} \sim 1$ , the incipient secondary recompression locus appears to behave as a corresponding states parameter but at the lower temperatures and  $P_{R_0} < 1$ , it does not. The approach may need to be modified to accommodate changes in friction factor. Here, we find (see also eqs. (5) and (6))

$$P_{R_0} = 5 T_{R_0}^{4.3} \quad \text{p-hydrogen}$$

$$P_{R_0} = 3.68 T_{R_0}^7 \quad \text{nitrogen}$$

Similar results were found for the Borda inlet geometry, reference 4, and an approximate locus representing those data is given on figure 19. The trend appears in the data of figure 19, but system control at these low pressures is difficult, sensitivity is lower, and the backpressure becomes a significant part of the free jet pressure. The free jet might be expanded through a longer L/D tube (lower effective L/D) if the tube were exhausted into a vacuum.

While unresolved it appears that the effective L/D of eq. (6) should be increased by 30 percent, and fluid jets do not follow conventional corresponding states very well.

#### SYMBOLS

A	area, $\text{cm}^2$
C	constant of eq. (5)
$C_1$	constant of eq. (6)
D	tube diameter, cm
G	flow rate, $\text{g}/\text{cm}^2\text{-s}$
$G_R$	reduced flow rate, $G = G/G^*$
$G^*$	flow normalizing parameter, $\sqrt{P_c \rho_c / Z_c}$ , 6010 $\text{g}/\text{cm}^2\text{-s}$ , for nitrogen; 1158 $\text{g}/\text{cm}^2\text{-s}$ , for hydrogen
L	tube length, cm
$L_1$	extension length, cm
P	pressure, MPa

$\bar{P}$	$(P_{o_1} + P_{o_2})/2$ average pressure, MPa
$P_R$	reduced pressure, $P/P_c$
$R$	gas constant, $\text{MPa}\cdot\text{cm}^3/\text{g}\cdot\text{K}$
$T$	temperature, K
$T_R$	reduced temperature, $T/T_c$
$V$	specific volume, $\text{cm}^3/\text{g}$
$Z$	compressibility, $PV/RT$
$\rho$	density, $\text{g}/\text{cm}^3$
$\epsilon$	surface roughness ratio
Subscripts:	
$c$	critical
$o$	stagnation
$sat$	saturation
1, 18	pressure tap locations

### SUMMARY

In this paper, the effects of free jet phenomena, jetting, in a  $90^\circ$ -sharp edge inlet tube have been established and comparisons made to jetting in tubes with Borda type inlets.

1. Jetting can occur when the inlet stagnation pressures are greater than the pressure defined by the incipient secondary recompression locus for both the  $90^\circ$ -sharp edge orifice tube and the Borda type inlets. For smooth tubes, these loci are defined by

$$P_{R_o} = C(L/D, \epsilon) T_{R_o}^n$$

where

$$C(L/D, \epsilon) = C_1 (L/D)^m$$

For fluid nitrogen data, the selected values of  $n$ ,  $m$  and  $C_1$  are  $n = 7$ ,  $m = 2.5$ ,

$$C_1 = 1.8 \times 10^{-4} \quad 90^\circ\text{-sharp edge inlet}$$

$$C_1 = 1.7 \times 10^{-4} \quad \text{Borda type inlet}$$

To use this relation for fluid hydrogen, it appears that the actual L/D should be increased by 30 percent, but the question is not yet resolved. For specific results, consult figure 19.

2. The mass flux in the  $90^\circ$ -sharp edge inlet tubes are perhaps 5 percent larger than for the Borda inlet tubes at  $T_{R_0} < 1$ , but nearly the same near  $T_{R_0} = 1$ .

3. Using fluids nitrogen and hydrogen, the 53 L/D  $90^\circ$ -sharp edge inlet and Borda type inlet tube results, and the principle of corresponding states, the following four propositions are offered, the first three of which are extensions of reference 4:

a. The free jet phenomena appear to be common to all simple fluids in tubes with inlets ranging from  $90^\circ$ -sharp edge to the Borda type inlets with the primary control at the inlet.

b. The phenomena are completely characterized by inlet stagnation conditions and tube geometry.

c. The reduced critical mass flux,  $G_R = G/G^*$ , follows the applied corresponding states principles and results attained for fluid nitrogen (or hydrogen) are applicable to all simple fluids. The latter implies that using fluid hydrogen results, the range of applicability of  $G_R$  for fluid nitrogen can be at least doubled, e.g., to  $P_{R_0} = 6$  for  $T_{R_0} = 0.67$ .

d. The pressure profiles, while similar, possess a different locus of secondary recompression for hydrogen than for nitrogen indicating that the extended principle may be required and surface roughness needs to be assessed before a law of correspondence can be established. Also the free jet expansion of hydrogen into a "vacuum" may also be required to establish the locus.

#### REFERENCES

1. Birkhoff, G., and Zarantonello, E. H. (1957), *Jets, Wakes, and Cavities*, Applied Mathematics and Mechanics, Vol. II (Academic Press, New York).
2. Gurevich, M. I. (1965), *Theory of Jets in Ideal Fluids* (Academic Press, New York).
3. Hendricks, R. C., and Simoneau, R. J. (1978), *Some Flow Phenomena in a Constant Area Duct with a Borda Type Inlet Including the Critical Region*, ASME Paper 78-WA/HT-37 (ASME, New York).

4. Hendricks, R. C. (1979), Some Aspects of a Free Jet Phenomena to 105 L/D in a Constant Area Duct, NASA TM-79050 (NASA, Washington, D. C.).
5. Hendricks, R. C., et al. (1966), Experimental Heat Transfer Results for Cryogenic Hydrogen Flowing in Tubes at Subcritical and Supercritical Pressures to 800 Pounds-Per Square Inch Absolute, NASA TN D-3095 (NASA, Washington, D. C.).
6. Hendricks, R. C., and Poolos, N. P. (1979), Critical Mass Flux Through Short Borda Type Inlets of Various Cross Sections, NASA TM-79017 (NASA, Washington, D. C.).
7. Hendricks, R. C. (1974), Normalizing Parameters for the Critical Flow Rate of Simple Fluids through Nozzles, Proc. of Fifth Int. Cryogenic Engr. Conf., Kyoto, Japan, May 1974. See also NASA TM X-71545 (NASA, Washington, D. C.).
8. Hendricks, R. C., and Simoneau, R. J. (1973), Application of the Principle of Corresponding States to Two-Phase Choked Flow, NASA TM X-68193 (NASA, Washington, D. C.).
9. Hendricks R. C., Simoneau, R. J., and Barrows, R. F. (1976), Two-Phase Choked Flow of Subcooled Oxygen and Nitrogen, NASA TN D-8149 (NASA, Washington, D. C.).

TABLE I. - PRESSURE TAP LOCATIONS FOR 90° SHARP EDGE INLET TUBES<sup>b</sup>

Pressure tap	53 L/D		64 L/D		73 L/D		105 L/D	
	Location							
	cm	in.	cm	in.	cm	in.	cm	in.
	5.38	2.12	10.8	4.25	15.4	6.05	30.5	12
P <sub>0</sub>	Mixing chamber		Same location					
P <sub>01</sub>	Line at top of U		Same location					
<sup>a</sup> P <sub>02</sub>	-23.7	-9.34	-29.2	11.47	-33.8	-13.27	-45.9	-19.22
P <sub>1</sub>	-25.4	-9.98	-30.7	-12.08	-35.3	-13.88	-50.4	-19.8
P <sub>2</sub>	-24.7	-9.73	-30.1	-12.33	-34.7	-14.1	-49.8	-20.1
P <sub>3</sub>	-23.2	-9.12	-28.6	-11.25	-33.2	13.05	-48.3	-19.0
P <sub>4</sub>	-17.8	-7	P <sub>4</sub> - P <sub>18</sub> - the same for each L/D 					
P <sub>5</sub>	-15.2	-6						
P <sub>7</sub>	-10.2	-4						
P <sub>8</sub>	-7.6	-3						
P <sub>9</sub>	-5.1	-2						
P <sub>10</sub>	-2.5	-1						
P <sub>11</sub>	-1.3	-.5						
P <sub>12</sub>	-.64	-.125						
P <sub>13</sub>	-.32	-.125						
P <sub>14</sub>	.32	.125						
P <sub>15</sub>	.64	.25						
P <sub>16</sub>	1.3	.5						
P <sub>17</sub>	2.5	1						
P <sub>18</sub>	5.1	2						
P <sub>back</sub>	Immediately upstream of backpressure control valve for all test sections							

<sup>a</sup>At Sharp edge inlet.

<sup>b</sup>See also figure 2.

TABLE II. - DATA FOR FLUID NITROGEN FLOWING THROUGH A 53 L/D TUBE WITH A 90° SHARP EDGE INLET

Run no.	$\frac{v}{a}$	$\frac{v_0}{a}$	$P_0$	$P_{O_1}$	$P_{O_2}$	$P_1$	$P_2$	$P_3$	$P_4$	$P_5$	$P_6$	$P_7$	$P_8$	$P_9$	$P_{10}$	$P_{11}$	$P_{12}$	$P_{13}$	$P_{14}$	$P_{15}$	$P_{16}$	$P_{17}$	$P_{18}$	$P_{back}$	$T_m$	$T_a$	$S_p$	
2257	81.5	290.0	2.37	2.35	2.35	1.18	1.67	1.68	1.60	1.55	1.48	1.42	1.33	1.24	1.13	1.04	0.99	0.93	0.88	0.84	0.78	0.72	0.66	0.60	0.54	0.48	0.42	0.36
2258	137.0	253.0	4.63	4.00	4.02	1.96	2.83	2.87	2.73	2.62	2.51	2.41	2.26	2.13	1.93	1.78	1.69	1.58	1.50	1.42	1.34	1.26	1.18	1.10	1.02	0.94	0.86	0.78
2259	186.0	231.0	5.85	5.40	5.45	3.31	4.63	4.71	4.53	4.38	4.23	4.08	3.93	3.78	3.63	3.48	3.33	3.28	3.23	3.18	3.13	3.08	3.03	2.98	2.93	2.88	2.83	2.78
2260	235.0	210.0	6.32	6.00	6.05	3.81	5.28	5.38	5.18	5.00	4.83	4.66	4.49	4.32	4.15	3.98	3.81	3.64	3.47	3.30	3.13	2.96	2.79	2.62	2.45	2.28	2.11	1.94
2261	284.0	189.0	6.71	6.50	6.55	4.31	5.86	5.97	5.75	5.56	5.37	5.18	4.99	4.80	4.61	4.42	4.23	4.04	3.85	3.66	3.47	3.28	3.09	2.90	2.71	2.52	2.33	2.14
2262	333.0	168.0	7.10	7.00	7.05	4.81	6.31	6.43	6.20	6.00	5.80	5.60	5.40	5.20	5.00	4.80	4.60	4.40	4.20	4.00	3.80	3.60	3.40	3.20	3.00	2.80	2.60	2.40
2263	382.0	147.0	7.49	7.40	7.45	5.31	6.81	6.94	6.58	6.37	6.16	5.95	5.74	5.53	5.32	5.11	4.90	4.69	4.48	4.27	4.06	3.85	3.64	3.43	3.22	3.01	2.80	2.59
2264	431.0	126.0	7.88	7.80	7.85	5.81	7.31	7.45	7.00	6.78	6.56	6.34	6.12	5.90	5.68	5.46	5.24	5.02	4.80	4.58	4.36	4.14	3.92	3.70	3.48	3.26	3.04	2.82
2265	480.0	105.0	8.27	8.20	8.25	6.31	7.81	7.96	7.40	7.17	6.94	6.71	6.48	6.25	6.02	5.79	5.56	5.33	5.10	4.87	4.64	4.41	4.18	3.95	3.72	3.49	3.26	3.03
2266	529.0	84.0	8.66	8.60	8.65	6.81	8.31	8.47	7.80	7.56	7.32	7.08	6.84	6.60	6.36	6.12	5.88	5.64	5.40	5.16	4.92	4.68	4.44	4.20	3.96	3.72	3.48	3.24
2267	578.0	63.0	9.05	9.00	9.05	7.31	8.81	8.98	8.20	7.95	7.70	7.45	7.20	6.95	6.70	6.45	6.20	5.95	5.70	5.45	5.20	4.95	4.70	4.45	4.20	3.95	3.70	3.45
2268	627.0	42.0	9.44	9.40	9.45	7.81	9.31	9.49	8.60	8.34	8.08	7.82	7.56	7.30	7.04	6.78	6.52	6.26	6.00	5.74	5.48	5.22	4.96	4.70	4.44	4.18	3.92	3.66
2269	676.0	21.0	9.83	9.80	9.85	8.31	9.81	9.99	9.00	8.73	8.46	8.20	7.94	7.68	7.42	7.16	6.90	6.64	6.38	6.12	5.86	5.60	5.34	5.08	4.82	4.56	4.30	4.04
2270	725.0	0.0	10.22	10.20	10.25	8.81	10.31	10.50	9.60	9.32	9.05	8.78	8.51	8.24	7.97	7.70	7.43	7.16	6.90	6.64	6.38	6.12	5.86	5.60	5.34	5.08	4.82	4.56
2271	774.0	-19.0	10.61	10.60	10.65	9.31	10.81	11.00	10.10	9.81	9.53	9.25	8.97	8.70	8.43	8.16	7.89	7.62	7.35	7.08	6.81	6.54	6.27	6.00	5.73	5.46	5.19	4.92
2272	823.0	-38.0	11.00	11.00	11.05	9.81	11.31	11.50	10.60	10.30	10.01	9.73	9.45	9.17	8.90	8.63	8.36	8.09	7.82	7.55	7.28	7.01	6.74	6.47	6.20	5.93	5.66	5.39
2273	872.0	-57.0	11.39	11.40	11.45	10.31	11.61	11.80	10.90	10.60	10.31	10.02	9.74	9.46	9.18	8.90	8.62	8.34	8.06	7.78	7.50	7.22	6.94	6.66	6.38	6.10	5.82	5.54
2274	921.0	-76.0	11.78	11.80	11.85	10.81	12.11	12.30	11.40	11.10	10.81	10.52	10.23	9.94	9.65	9.36	9.07	8.78	8.49	8.20	7.91	7.62	7.33	7.04	6.75	6.46	6.17	5.88
2275	970.0	-95.0	12.17	12.20	12.25	11.31	12.41	12.60	11.70	11.40	11.11	10.82	10.53	10.24	9.95	9.66	9.37	9.08	8.79	8.50	8.21	7.92	7.63	7.34	7.05	6.76	6.47	6.18
2276	1019.0	-114.0	12.56	12.60	12.65	11.81	12.81	13.00	12.10	11.80	11.51	11.22	10.93	10.64	10.35	10.06	9.77	9.48	9.19	8.90	8.61	8.32	8.03	7.74	7.45	7.16	6.87	6.58
2277	1068.0	-133.0	12.95	13.00	13.05	12.31	13.11	13.30	12.40	12.10	11.81	11.52	11.23	10.94	10.65	10.36	10.07	9.78	9.49	9.20	8.91	8.62	8.33	8.04	7.75	7.46	7.17	6.88
2278	1117.0	-152.0	13.34	13.40	13.45	12.81	13.41	13.60	12.70	12.40	12.11	11.82	11.53	11.24	10.95	10.66	10.37	10.08	9.79	9.50	9.21	8.92	8.63	8.34	8.05	7.76	7.47	7.18
2279	1166.0	-171.0	13.73	13.80	13.85	13.31	13.61	13.80	12.90	12.60	12.31	12.02	11.73	11.44	11.15	10.86	10.57	10.28	9.99	9.70	9.41	9.12	8.83	8.54	8.25	7.96	7.67	7.38
2280	1215.0	-190.0	14.12	14.20	14.25	13.81	14.01	14.20	13.30	13.00	12.71	12.42	12.13	11.84	11.55	11.26	10.97	10.68	10.39	10.10	9.81	9.52	9.23	8.94	8.65	8.36	8.07	7.78
2281	1264.0	-209.0	14.51	14.60	14.65	14.31	14.41	14.60	13.70	13.40	13.11	12.82	12.53	12.24	11.95	11.66	11.37	11.08	10.79	10.50	10.21	9.92	9.63	9.34	9.05	8.76	8.47	8.18
2282	1313.0	-228.0	14.90	15.00	15.05	14.81	14.91	15.10	14.20	13.90	13.61	13.32	13.03	12.74	12.45	12.16	11.87	11.58	11.29	11.00	10.71	10.42	10.13	9.84	9.55	9.26	8.97	8.68
2283	1362.0	-247.0	15.29	15.40	15.45	15.31	15.41	15.60	14.70	14.40	14.11	13.82	13.53	13.24	12.95	12.66	12.37	12.08	11.79	11.50	11.21	10.92	10.63	10.34	10.05	9.76	9.47	9.18
2284	1411.0	-266.0	15.68	15.80	15.85	15.81	15.91	16.10	15.20	14.90	14.61	14.32	14.03	13.74	13.45	13.16	12.87	12.58	12.29	12.00	11.71	11.42	11.13	10.84	10.55	10.26	9.97	9.68
2285	1460.0	-285.0	16.07	16.20	16.25	16.21	16.31	16.50	15.60	15.30	15.01	14.72	14.43	14.14	13.85	13.56	13.27	12.98	12.69	12.40	12.11	11.82	11.53	11.24	10.95	10.66	10.37	10.08
2286	1509.0	-304.0	16.46	16.60	16.65	16.61	16.71	16.90	16.00	15.70	15.41	15.12	14.83	14.54	14.25	13.96	13.67	13.38	13.09	12.80	12.51	12.22	11.93	11.64	11.35	11.06	10.77	10.48
2287	1558.0	-323.0	16.85	17.00	17.05	17.01	17.11	17.30	16.40	16.10	15.81	15.52	15.23	14.94	14.65	14.36	14.07	13.78	13.49	13.20	12.91	12.62	12.33	12.04	11.75	11.46	11.17	10.88
2288	1607.0	-342.0	17.24	17.40	17.45	17.41	17.51	17.70	16.80	16.50	16.21	15.92	15.63	15.34	15.05	14.76	14.47	14.18	13.89	13.60	13.31	13.02	12.73	12.44	12.15	11.86	11.57	11.28
2289	1656.0	-361.0	17.63	17.80	17.85	17.81	17.91	18.10	17.20	16.90	16.61	16.32	16.03	15.74	15.45	15.16	14.87	14.58	14.29	14.00	13.71	13.42	13.13	12.84	12.55	12.26	11.97	11.68
2290	1705.0	-380.0	18.02	18.20	18.25	18.21	18.31	18.50	17.60	17.30	17.01	16.72	16.43	16.14	15.85	15.56	15.27	14.98	14.69	14.40	14.11	13.82	13.53	13.24	12.95	12.66	12.37	12.08
2291	1754.0	-400.0	18.41	18.60	18.65	18.61	18.71	18.90	18.00	17.70	17.41	17.12	16.83	16.54	16.25	15.96	15.67	15.38	15.09	14.80	14.51	14.22	13.93	13.64	13.35	13.06	12.77	12.48
2292	1803.0	-419.0	18.80	19.00	19.05	19.01	19.11	19.30	18.40	18.10	17.81	17.52	17.23	16.94	16.65	16.36	16.07	15.78	15.49	15.20	14.91	14.62	14.33	14.04	13.75	13.46	13.17	12.88
2293	1852.0	-438.0	19.19	19.40	19.45	19.41	19.51	19.70	18.80	18.50	18.21	17.92	17.63	17.34	17.05	16.76	16.47	16.18	15.89	15.60	15.31	15.02	14.73	14.44	14.15	13.86	13.57	13.28
2294	1901.0	-457.0	19.58	19.80	19.85	19.81	19.91	20.10	19.20	18.90	18.61	18.32	18.03	17.74	17.45	17.16	16.87	16.58	16.29	16.00	15.71	15.42	15.13	14.84	14.55	14.26	13.97	13.68
2295	1950.0	-476.0	19.97	20.20	20.25	20.21	20.31	20.50	19.60	19.30	19.01	18.72	18.43	18.14	17.85	17.56	17.27	16.98	16.69	16.40	16.11	15.82	15.53	15.24	14.95	14.66	14.37	14.08
2296	2000.0	-495.0	20.36	20.60	20.65	20.61	20.71	20.90	20.00	19.70	19.41	19.12	18.83	18.54	18.25	17.96	17.67	17.38	17.09	16.80	16.51	16.22	15.93	15.64	15.35	15.06	14.77	14.48
2297	2049.0	-514.0	20.75	21.00	21.05	21.01	21.11	21.30	20.40	20.10	19.81	19.52	19.23	18.94	18.65	18.36	18.07	17.78	17.49	17.20	16.91	16.62	16.33	16.04	15.75	15.46	15.17	14.88
2298	2098.0	-533.0	21.14	21.40	21.45	21.41	21.51	21.70	20.80	20.50	20.21	19.92	19.63	19.34	19.05	18.76	18.47	18.18	17.89	17.60	17.31	17.02	16.73	16.44	16.15	15.86	15.57	15.28
2299	2147.0	-552.0	21.53	21.80	21.85																							



TABLE IV. - DATA FOR FLUID NITROGEN FLOWING THROUGH A 73 L/D TUBE WITH A 90° SHARP EDGE INLET

Run No.	$T_0$	$T_1$	$T_2$	$T_3$	$T_4$	$T_5$	$T_6$	$T_7$	$T_8$	$T_9$	$T_{10}$	$T_{11}$	$T_{12}$	$T_{13}$	$T_{14}$	$T_{15}$	$T_{16}$	$T_{17}$	$T_{18}$	$T_{19}$	$T_{20}$	$T_{21}$	$T_{back}$	$T_R$	$T_A$	$C_R$	
2-1	958.0	88.0	5.59	5.82	5.86	0.12	0.14	0.24	0.30	0.30	0.31	0.32	0.33	0.34	0.32	0.35	0.25	0.21	0.15	0.42	0.27	0.27	0.32	0.32	0.597	1.591	0.972
2371	817.0	87.6	4.09	3.99	4.02	0.13	0.14	0.23	0.30	0.29	0.31	0.30	0.32	0.33	0.32	0.25	0.28	0.25	0.13	0.15	0.32	0.27	0.27	0.31	0.698	1.175	0.783
2372	546.0	87.4	2.72	2.68	2.66	0.16	0.15	0.23	0.31	0.30	0.31	0.30	0.32	0.33	0.32	0.28	0.25	0.21	0.16	0.28	0.27	0.28	0.31	0.692	0.772	0.95	
2373	519.0	86.5	2.23	2.17	2.17	0.16	0.15	0.23	0.30	0.29	0.30	0.29	0.32	0.33	0.32	0.28	0.25	0.21	0.16	0.28	0.27	0.28	0.30	0.688	0.835	0.54	
2374	411.0	86.9	1.74	1.69	1.69	0.15	0.16	0.23	0.30	0.29	0.30	0.29	0.32	0.33	0.32	0.28	0.25	0.21	0.16	0.28	0.27	0.27	0.30	0.688	0.835	0.54	
2375	411.0	87.2	1.23	1.19	1.18	0.17	0.17	0.24	0.30	0.29	0.30	0.29	0.32	0.33	0.32	0.28	0.25	0.21	0.16	0.28	0.27	0.27	0.30	0.688	0.835	0.54	
2376	355.0	87.0	6.36	5.22	5.28	0.27	0.31	0.59	0.81	0.81	0.84	0.84	0.85	1.00	1.01	0.95	0.95	0.89	0.62	0.60	0.61	0.61	0.61	0.61	0.61	0.61	
2377	329.0	87.0	5.93	5.80	5.85	0.29	0.33	0.59	0.81	0.81	0.84	0.84	0.85	1.00	1.01	0.95	0.95	0.89	0.62	0.60	0.61	0.61	0.61	0.61	0.61	0.61	
2378	275.0	103.0	4.18	4.09	4.12	0.38	0.38	0.62	0.88	0.88	0.91	0.91	1.13	1.20	1.08	0.99	0.98	0.93	0.69	0.68	0.68	0.68	0.68	0.68	0.68	0.68	
2379	385.0	103.0	2.58	2.53	2.58	0.56	0.72	1.03	1.39	1.44	1.35	1.25	1.13	1.07	1.08	0.96	0.96	0.92	0.69	0.68	0.68	0.68	0.68	0.68	0.68	0.68	
2380	331.0	99.7	3.78	3.62	3.68	0.25	0.28	0.47	0.66	0.72	0.72	0.72	0.72	0.72	0.72	0.72	0.72	0.72	0.72	0.72	0.72	0.72	0.72	0.72	0.72	0.72	
2381	302.0	101.0	5.15	5.04	5.08	0.27	0.30	0.51	0.70	0.76	0.76	1.12	1.03	0.91	0.80	0.81	0.78	0.57	0.56	0.56	0.56	0.56	0.56	0.56	0.56	0.56	
2382	308.0	96.0	5.76	5.63	5.65	0.20	0.22	0.42	0.63	0.75	0.74	1.36	1.27	1.12	1.03	0.91	0.84	0.84	0.78	0.57	0.56	0.56	0.56	0.56	0.56	0.56	
2383	263.0	96.4	4.96	4.88	4.88	0.22	0.24	0.42	0.63	0.75	0.74	1.36	1.27	1.12	1.03	0.91	0.84	0.84	0.78	0.57	0.56	0.56	0.56	0.56	0.56	0.56	
2384	263.0	96.5	4.39	4.20	4.23	0.25	0.25	0.45	0.65	0.75	0.75	1.36	1.27	1.12	1.03	0.91	0.84	0.84	0.78	0.57	0.56	0.56	0.56	0.56	0.56	0.56	
2385	266.0	96.7	3.80	3.71	3.74	0.25	0.25	0.45	0.65	0.75	0.75	1.36	1.27	1.12	1.03	0.91	0.84	0.84	0.78	0.57	0.56	0.56	0.56	0.56	0.56	0.56	
2386	266.0	96.7	3.80	3.71	3.74	0.25	0.25	0.45	0.65	0.75	0.75	1.36	1.27	1.12	1.03	0.91	0.84	0.84	0.78	0.57	0.56	0.56	0.56	0.56	0.56	0.56	
2387	493.0	95.8	1.34	1.35	1.35	0.34	0.34	0.54	0.74	0.74	0.74	1.13	1.07	0.91	0.80	0.80	0.78	0.57	0.56	0.56	0.56	0.56	0.56	0.56	0.56	0.56	
2388	493.0	95.8	1.34	1.35	1.35	0.34	0.34	0.54	0.74	0.74	0.74	1.13	1.07	0.91	0.80	0.80	0.78	0.57	0.56	0.56	0.56	0.56	0.56	0.56	0.56	0.56	
2389	73.0	92.1	3.47	3.32	3.40	0.17	0.18	0.30	0.40	0.39	0.41	0.40	0.42	0.43	0.46	0.45	0.45	0.45	0.45	0.45	0.45	0.45	0.45	0.45	0.45	0.45	
2390	73.0	92.1	3.47	3.32	3.40	0.17	0.18	0.30	0.40	0.39	0.41	0.40	0.42	0.43	0.46	0.45	0.45	0.45	0.45	0.45	0.45	0.45	0.45	0.45	0.45	0.45	
2391	52.0	92.9	3.03	2.95	2.97	0.21	0.21	0.35	0.47	0.46	0.49	0.47	0.45	0.48	0.47	0.47	0.47	0.47	0.47	0.47	0.47	0.47	0.47	0.47	0.47	0.47	
2392	430.0	92.6	1.72	1.29	1.29	0.30	0.30	0.50	0.70	0.70	0.70	1.13	1.07	0.91	0.80	0.80	0.78	0.57	0.56	0.56	0.56	0.56	0.56	0.56	0.56	0.56	
2393	430.0	92.6	1.72	1.29	1.29	0.30	0.30	0.50	0.70	0.70	0.70	1.13	1.07	0.91	0.80	0.80	0.78	0.57	0.56	0.56	0.56	0.56	0.56	0.56	0.56	0.56	
2394	750.0	91.3	2.97	2.90	2.91	0.11	0.11	0.18	0.22	0.22	0.22	0.22	0.22	0.22	0.22	0.22	0.22	0.22	0.22	0.22	0.22	0.22	0.22	0.22	0.22	0.22	
2395	583.0	91.3	2.97	2.90	2.91	0.11	0.11	0.18	0.22	0.22	0.22	0.22	0.22	0.22	0.22	0.22	0.22	0.22	0.22	0.22	0.22	0.22	0.22	0.22	0.22	0.22	
2396	583.0	91.3	2.97	2.90	2.91	0.11	0.11	0.18	0.22	0.22	0.22	0.22	0.22	0.22	0.22	0.22	0.22	0.22	0.22	0.22	0.22	0.22	0.22	0.22	0.22	0.22	
2397	583.0	91.3	2.97	2.90	2.91	0.11	0.11	0.18	0.22	0.22	0.22	0.22	0.22	0.22	0.22	0.22	0.22	0.22	0.22	0.22	0.22	0.22	0.22	0.22	0.22	0.22	
2398	583.0	91.3	2.97	2.90	2.91	0.11	0.11	0.18	0.22	0.22	0.22	0.22	0.22	0.22	0.22	0.22	0.22	0.22	0.22	0.22	0.22	0.22	0.22	0.22	0.22	0.22	
2399	583.0	91.3	2.97	2.90	2.91	0.11	0.11	0.18	0.22	0.22	0.22	0.22	0.22	0.22	0.22	0.22	0.22	0.22	0.22	0.22	0.22	0.22	0.22	0.22	0.22	0.22	
2400	583.0	91.3	2.97	2.90	2.91	0.11	0.11	0.18	0.22	0.22	0.22	0.22	0.22	0.22	0.22	0.22	0.22	0.22	0.22	0.22	0.22	0.22	0.22	0.22	0.22	0.22	
2401	583.0	91.3	2.97	2.90	2.91	0.11	0.11	0.18	0.22	0.22	0.22	0.22	0.22	0.22	0.22	0.22	0.22	0.22	0.22	0.22	0.22	0.22	0.22	0.22	0.22	0.22	
2402	583.0	91.3	2.97	2.90	2.91	0.11	0.11	0.18	0.22	0.22	0.22	0.22	0.22	0.22	0.22	0.22	0.22	0.22	0.22	0.22	0.22	0.22	0.22	0.22	0.22	0.22	
2403	583.0	91.3	2.97	2.90	2.91	0.11	0.11	0.18	0.22	0.22	0.22	0.22	0.22	0.22	0.22	0.22	0.22	0.22	0.22	0.22	0.22	0.22	0.22	0.22	0.22	0.22	
2404	583.0	91.3	2.97	2.90	2.91	0.11	0.11	0.18	0.22	0.22	0.22	0.22	0.22	0.22	0.22	0.22	0.22	0.22	0.22	0.22	0.22	0.22	0.22	0.22	0.22	0.22	
2405	583.0	91.3	2.97	2.90	2.91	0.11	0.11	0.18	0.22	0.22	0.22	0.22	0.22	0.22	0.22	0.22	0.22	0.22	0.22	0.22	0.22	0.22	0.22	0.22	0.22	0.22	
2406	583.0	91.3	2.97	2.90	2.91	0.11	0.11	0.18	0.22	0.22	0.22	0.22	0.22	0.22	0.22	0.22	0.22	0.22	0.22	0.22	0.22	0.22	0.22	0.22	0.22	0.22	
2407	583.0	91.3	2.97	2.90	2.91	0.11	0.11	0.18	0.22	0.22	0.22	0.22	0.22	0.22	0.22	0.22	0.22	0.22	0.22	0.22	0.22	0.22	0.22	0.22	0.22	0.22	

ORIGINAL PAGE IS OF POOR QUALITY





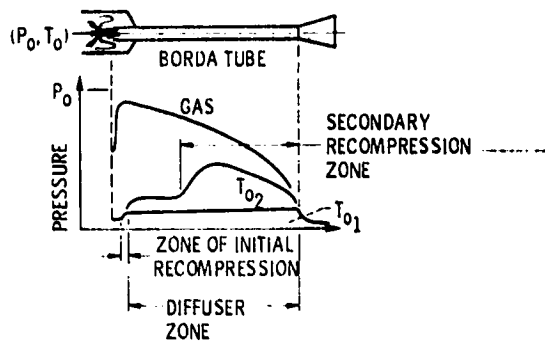


Figure 1. - Sketch of pressure profiles which characterize the Borda tube. Data of references 3 and 4.

E-131

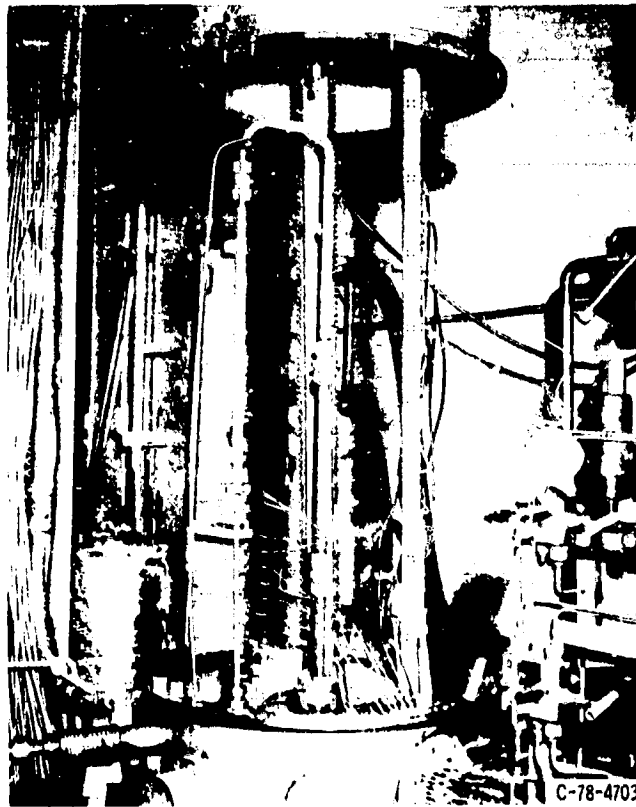
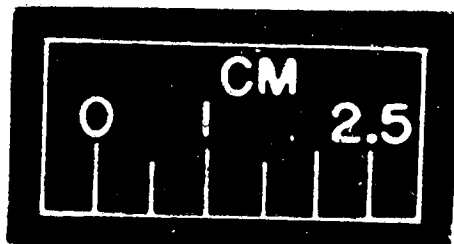
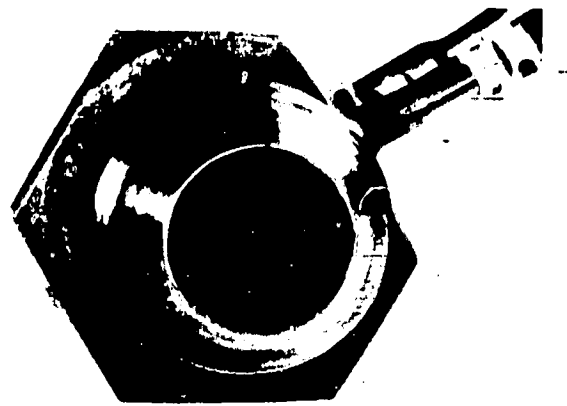


Figure 2. - Apparatus.

ORIGINAL PAGE IS  
OR OI



C-79-535

Figure 3. - Sharp edge inlet.

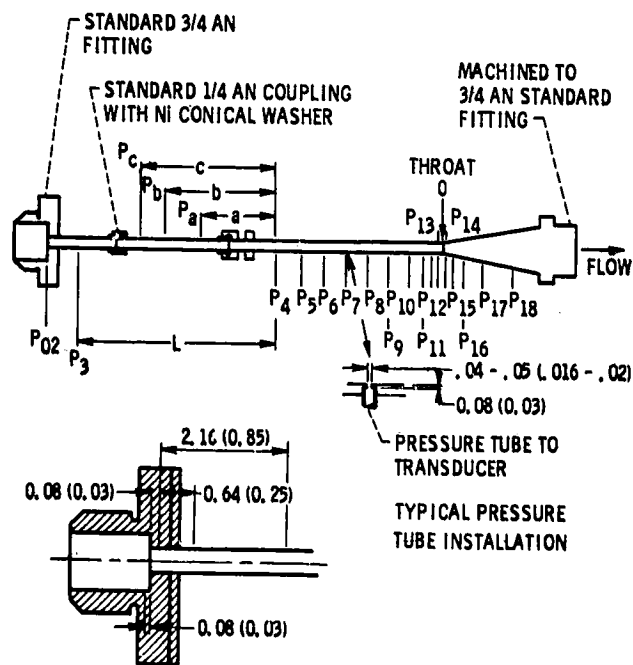
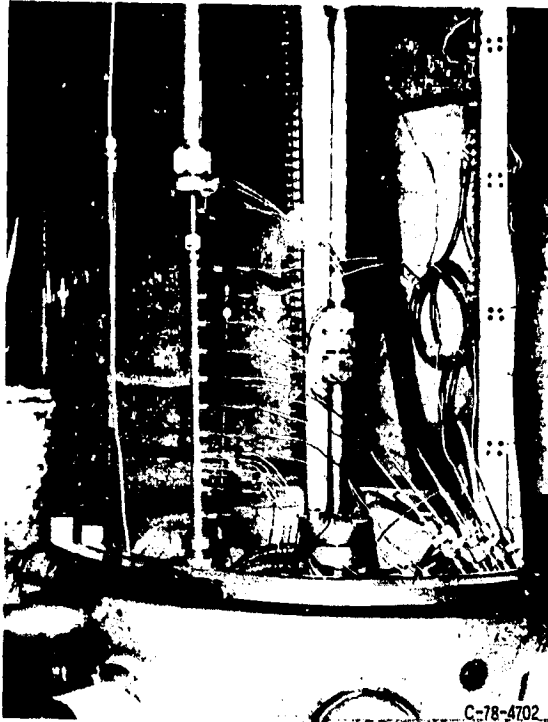
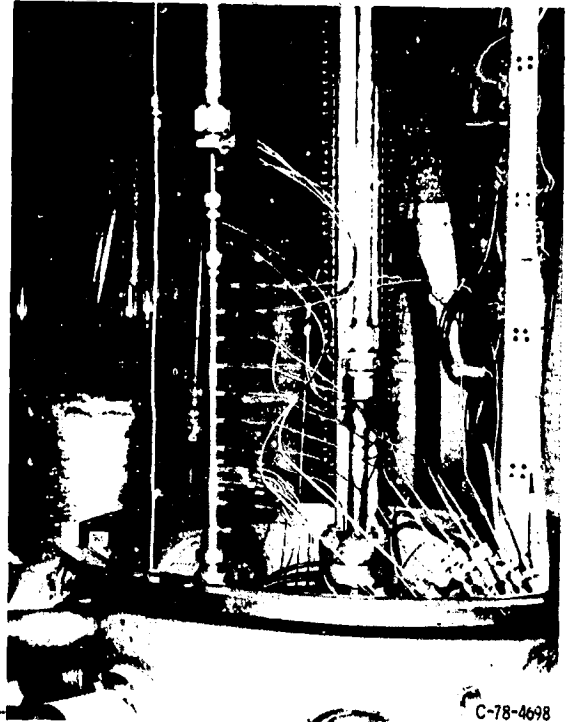


Figure 4. - Schematic of 90° - sharp edge inlet test section.  
See table I for pressure tap locations and dimensions.



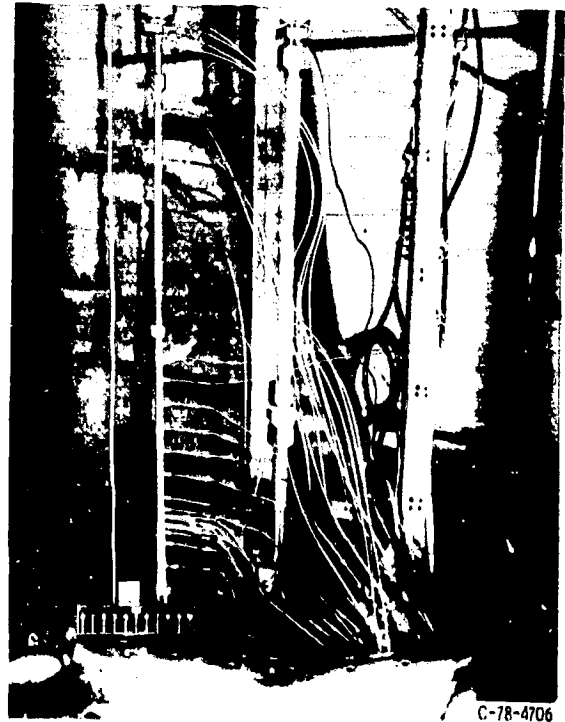
(a) L/D=53



(b) L/D=64



(c) L/D=73



(d) L/D=105

Figure 5. - Installed test sections.

ORIGINAL PART  
OF POOR QUALITY

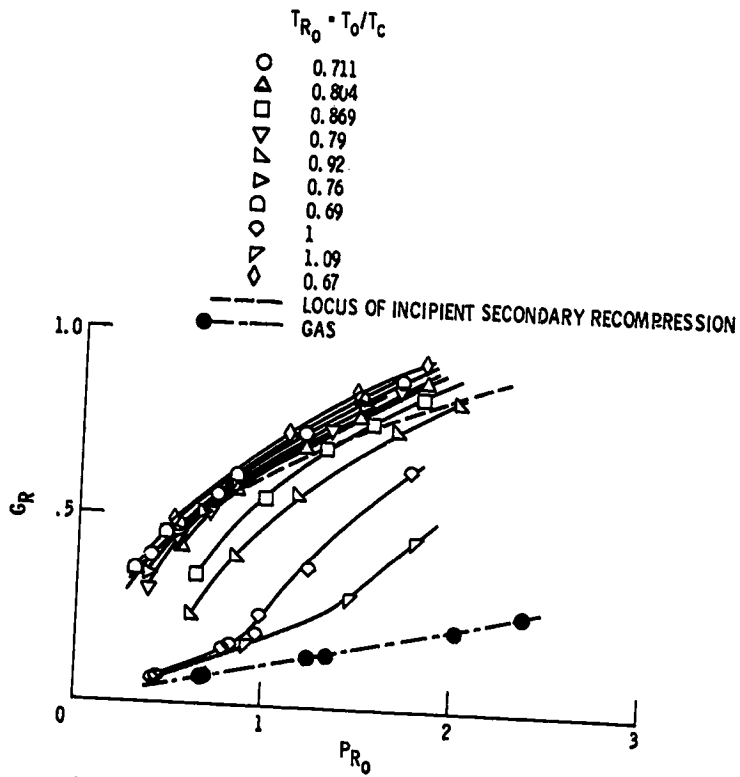


Figure 6. - Reduced critical mass flux for 90° sharp edge tubes as a function of reduced inlet stagnation pressure for selected isotherms using fluid nitrogen with  $U/D = 53$ .

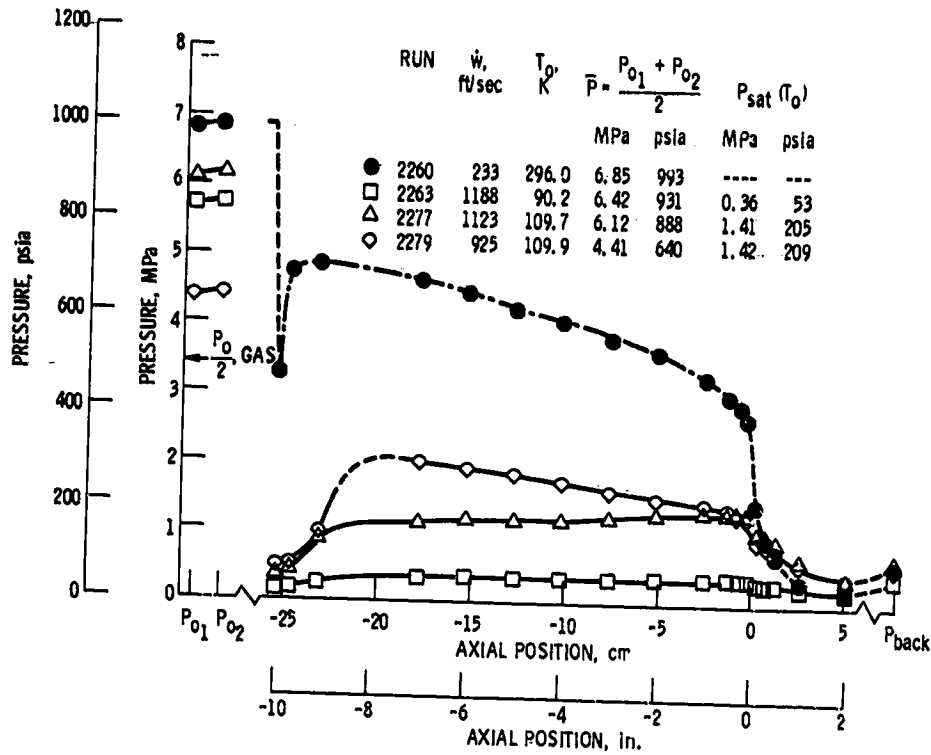


Figure 7. - Axial pressure profiles for 90° sharp edge inlet tubes illustrating incipient secondary recompression using fluid nitrogen for  $L/D = 53$ .

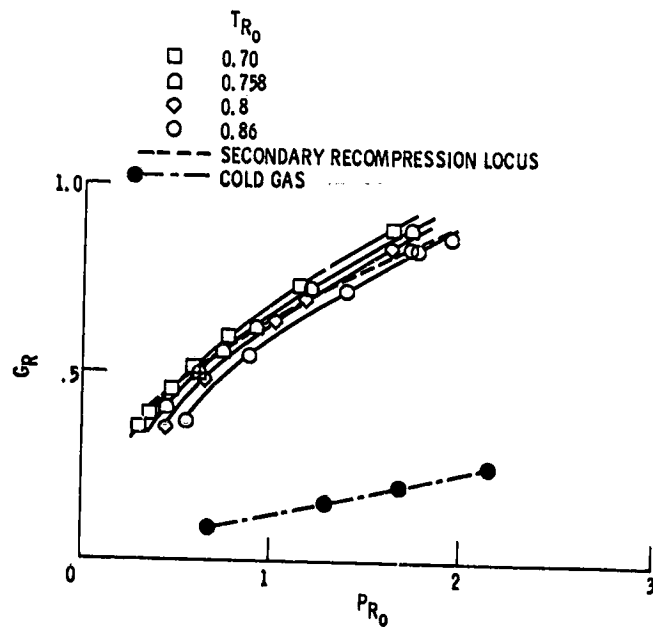


Figure 8. - Reduced critical mass flux for 90° sharp edge tubes as a function of reduced inlet stagnation pressure for selected isotherms using fluid nitrogen with  $L/D = 64$ .

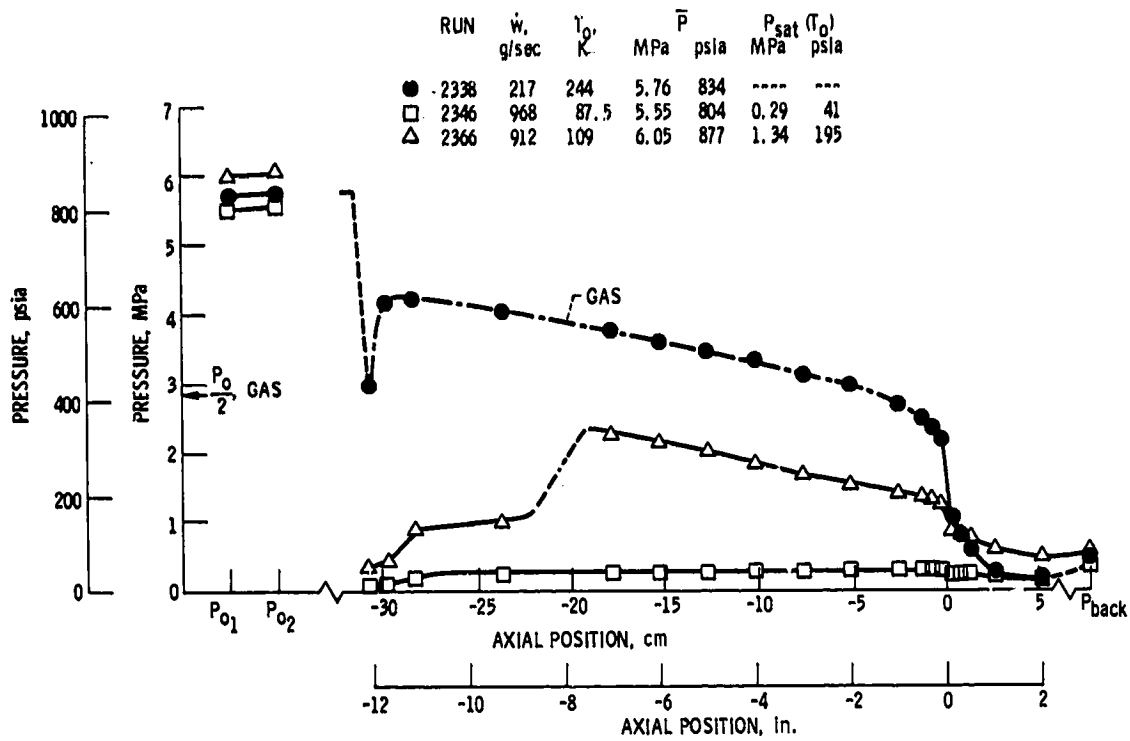


Figure 9. - Axial pressure profiles for  $90^\circ$  sharp edge inlet tubes illustrating incipient secondary recompression using fluid nitrogen for  $L/D = 64$ .

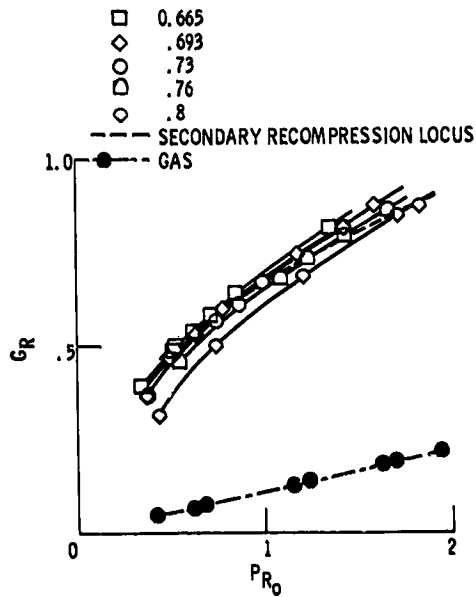


Figure 10. - Reduced critical mass flux for  $90^\circ$  sharp edge tubes as a function of reduced inlet stagnation pressure for selected isotherms using fluid nitrogen with  $L/D = 73$ .

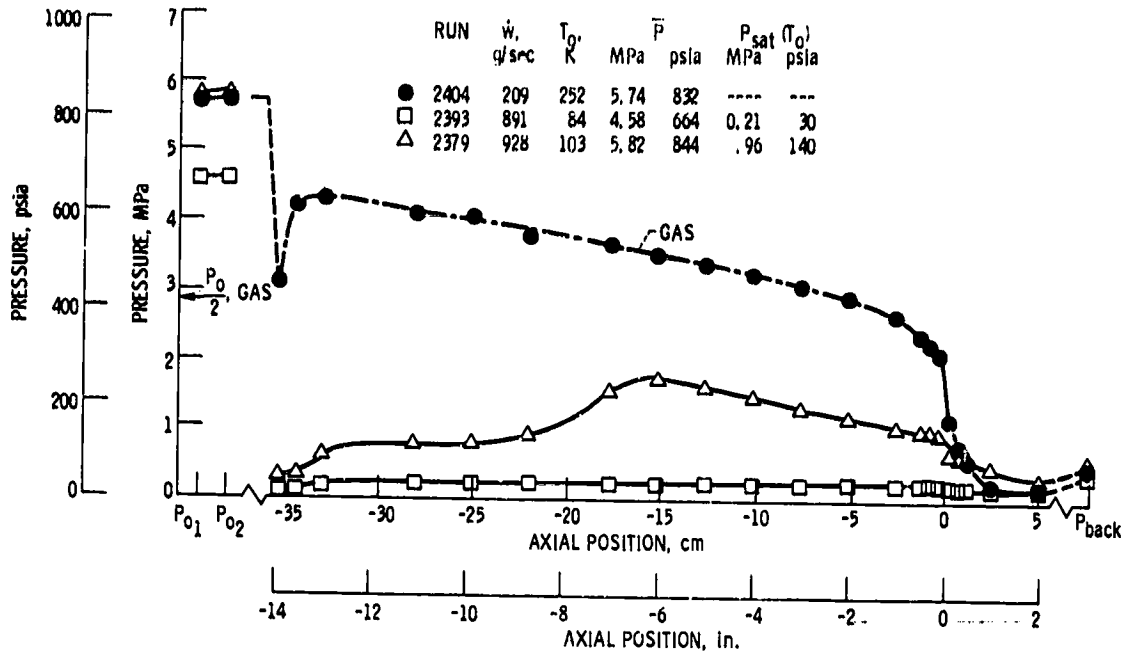


Figure 11. - Axial pressure profiles for 90° sharp edge inlet tubes illustrating incipient secondary recompression using fluid nitrogen for L/D = 73.

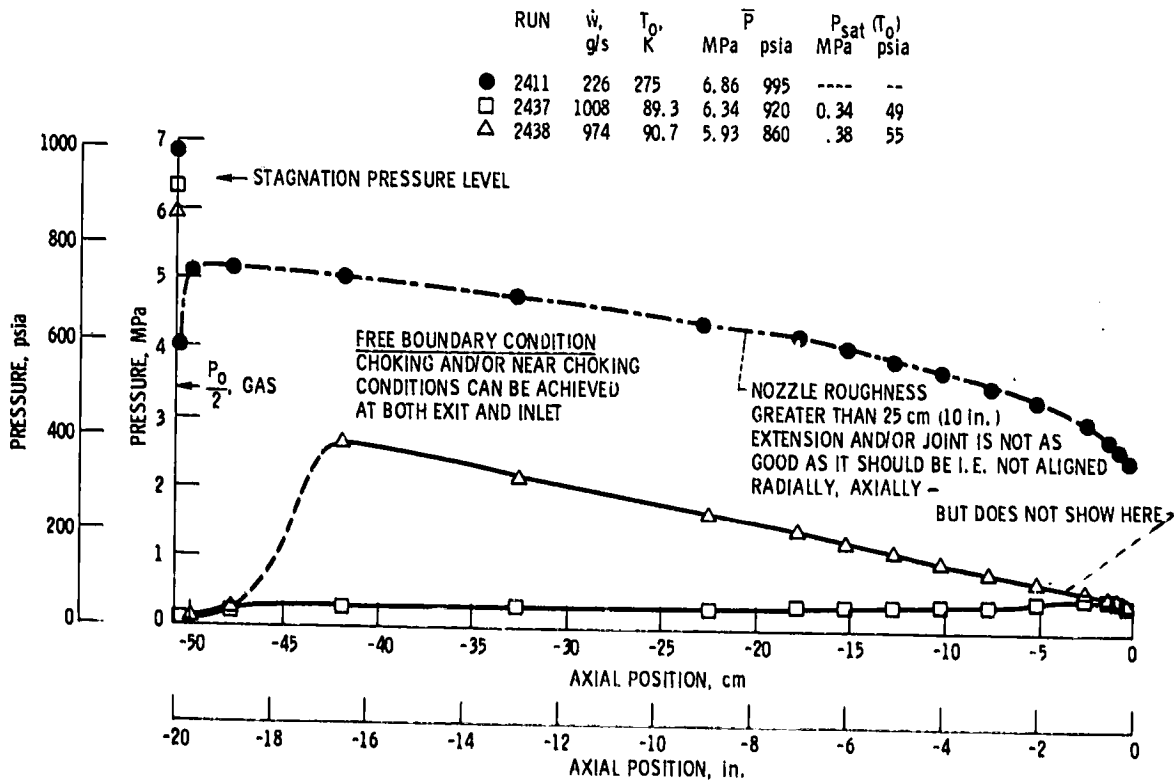


Figure 12. - Axial pressure profiles for 90° sharp edge inlet tubes illustrating incipient secondary recompression using fluid nitrogen for L/D = 105.

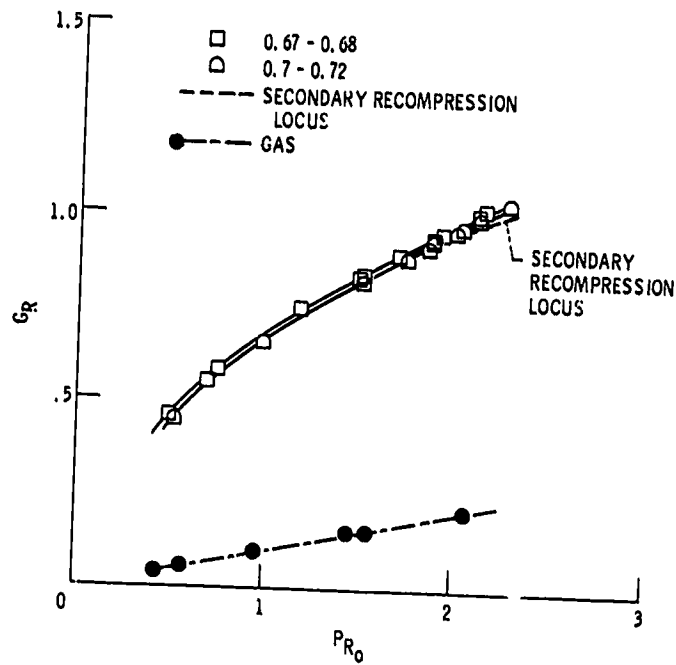


Figure 13. - Reduced critical mass flux for 90° sharp edge tubes as a function of reduced inlet stagnation pressure for selected isotherms using fluid nitrogen with  $L/D = 105$ .

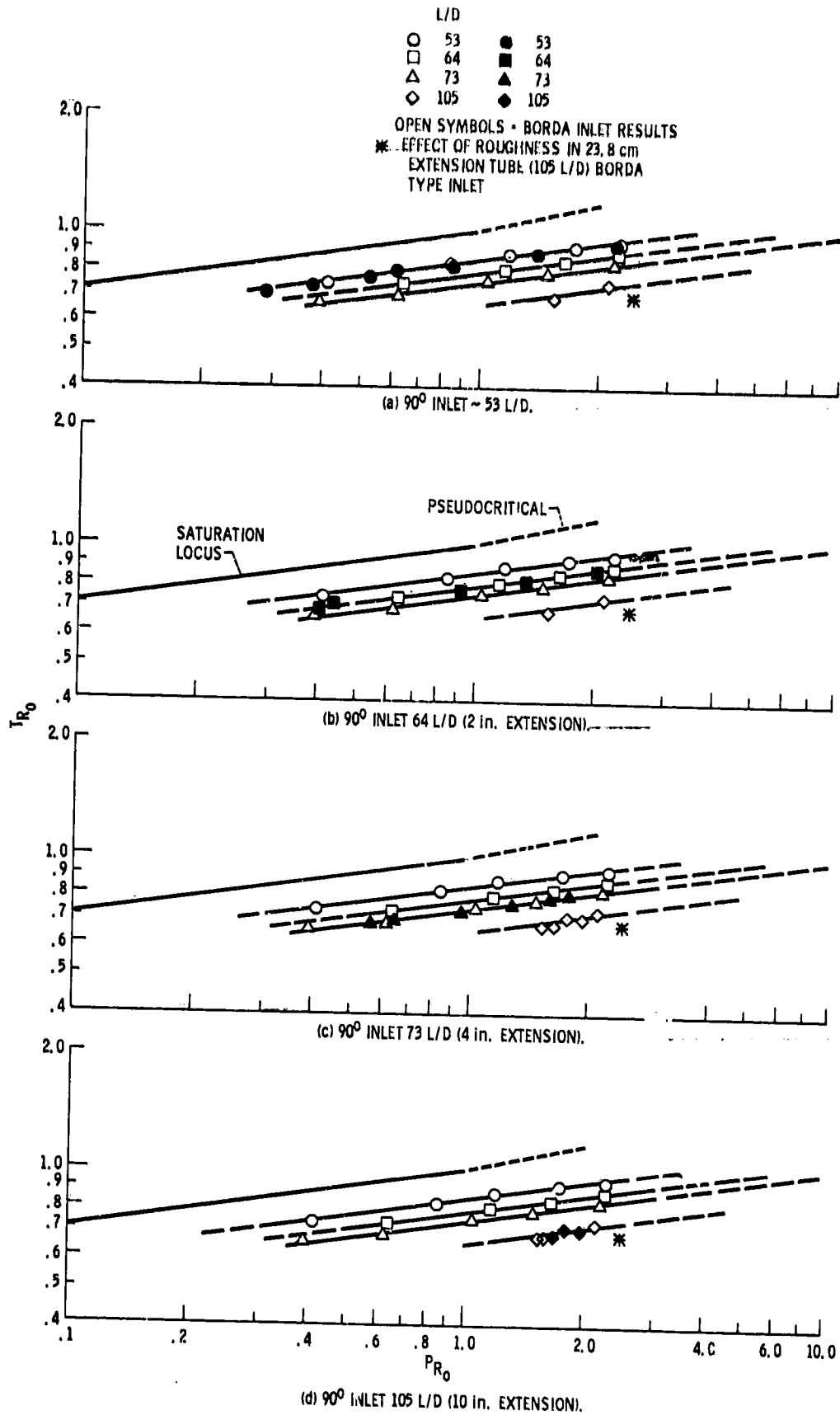


Figure 14. - Loci of incipient secondary recompression in tubes with 90° sharp edge and Borda type inlets.

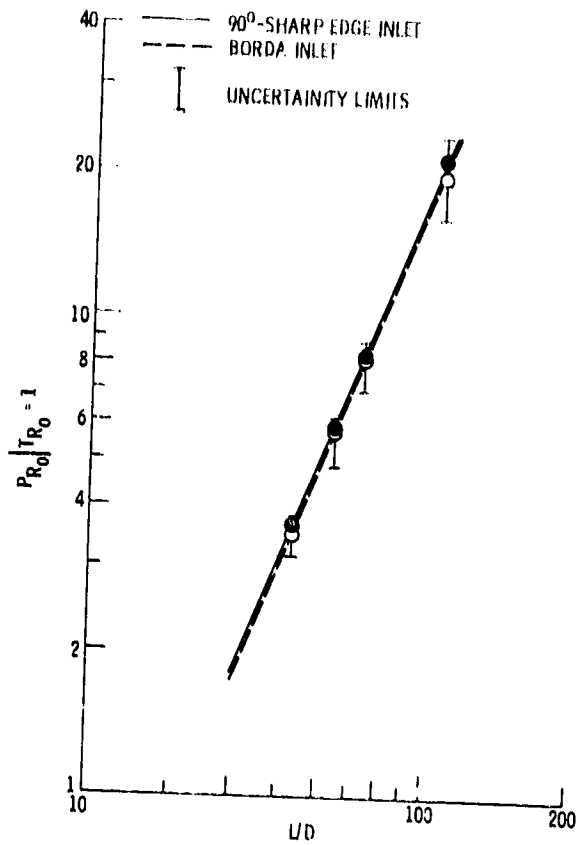


Figure 15. - Intercept values at  $T_{R_0} = 1$  for incipient secondary recompression in  $90^\circ$  and Borda tubes as a function of  $L/D$ .

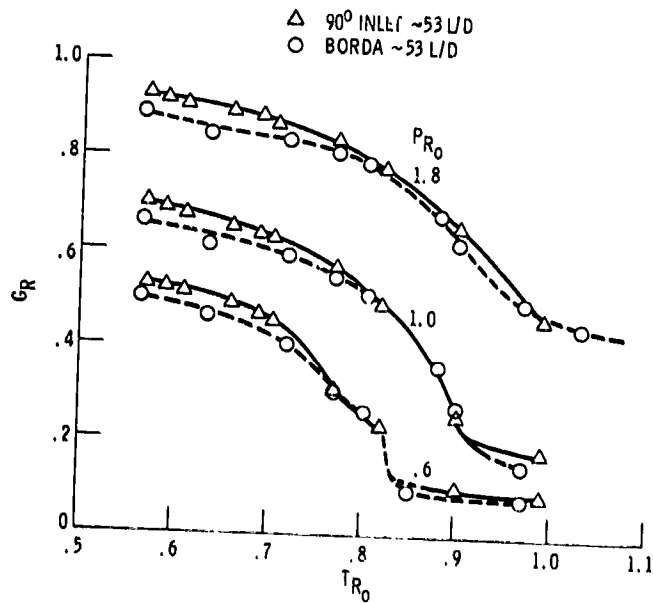


Figure 16. - Comparison of reduced mass flux as a function of reduced temperature for tubes with  $90^\circ$  sharp edge and Borda type inlets.

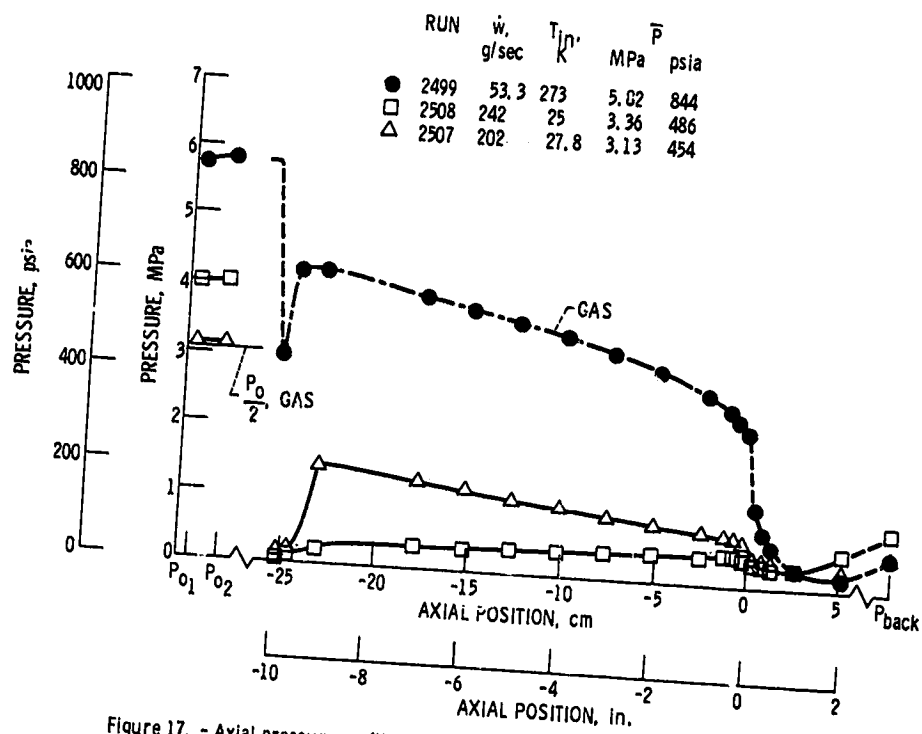


Figure 17. - Axial pressure profiles for fluid hydrogen in a 53 L/D 90° sharp edge inlet.

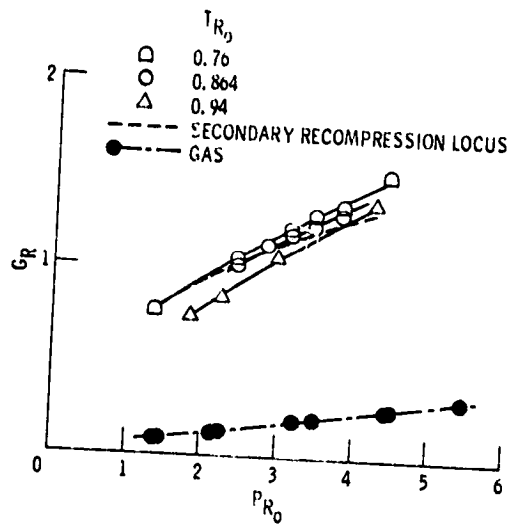


Figure 18. - Reduced critical mass flux for fluid hydrogen in a 53 l/D 90° sharp edge inlet as a function of reduced inlet stagnation pressure for selected isotherms.

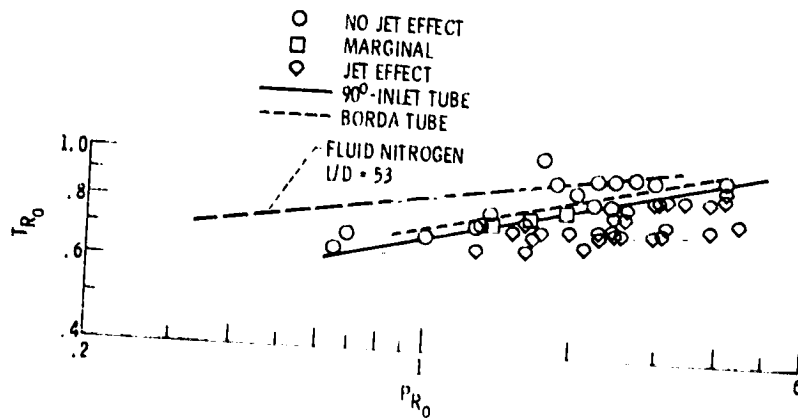


Figure 19. - Fluid jet effects for p-hydrogen in 53 l/D 90° sharp edge inlet tube.